ELSEVIER

Journal of Nuclear Materials 313–316 (2003) 199–203

journal of nuclear materials

www.elsevier.com/locate/jnucmat

Impurity effects and temperature dependence of D retention in single crystal tungsten

M. Poon *, A.A. Haasz, J.W. Davis, R.G. Macaulay-Newcombe

Fusion Research Group, University of Toronto Institute for Aerospace Studies, 4925 Dufferin Street, Toronto, Ont., Canada M3H 5T6

Abstract

Deuterium retention in single crystal tungsten was measured as a function of implantation temperature (300–700 K), fluence (10^{21}–10^{25} D^+/m^2 s) and impurity levels for 500 eV/D^+ implantation. Prior to implantation, specimens were annealed under vacuum at temperatures up to 2200 K with the intention of reducing the impurity and defect contents. Secondary ion mass spectrometry measurements showed that near-surface carbon and oxygen levels decreased after annealing at 1775 K, but *increased* after annealing at 2200 K, and also increased after D^+ implantation. Thermal desorption spectra indicated that D retention increased with increasing D^+ fluence (with an apparent trend to saturation for implantation at 300 K), and decreased with increasing implant temperature. The desorption peaked at $T = 600$–900 K, depending on the implant fluence and temperature. There was little or no D retention for implantation at $T > 700$ K. C and O impurities are affected by the D^+ irradiation and appear to influence the D trapping mechanism and the amount of D retained.

PACS: 52.40.H
Keywords: Tungsten; Deuterium inventory; Hydrogen retention; Thermal desorption; Ion implantation; Hydrogen trapping

1. Introduction

Tungsten continues to receive attention as a candidate plasma-facing material because of its acceptable erosion properties at low plasma temperatures and its high-temperature strength. However, one of the concerns with tungsten, as with other plasma-facing materials, is its hydrogen transport and trapping properties. Available data indicate that hydrogen retention in tungsten is dependent on both the type of tungsten structure and the experimental parameters [1–10]. In order to understand the basic underlying mechanisms governing hydrogen interactions in tungsten, high purity single crystal tungsten, being almost completely free of grain boundaries and dislocations, is the ideal material to study. While single crystal tungsten will not be used in a fusion reactor, its study will help to determine the role of grain boundaries, impurities, vacancies, porosity and other material characteristics on hydrogen retention, recycling and permeation.

2. Experiment

2.1. Specimens

Several single crystal tungsten specimens, manufactured by the State Institute of Rare Metals, Moscow (hereafter labelled as 'M-SCW'), were provided by V.Kh. Alimov. The quoted purity of this material was 99.9 at.% with the main impurities being H (0.02 at.%), C (0.05 at.%) and O (0.05 at.%). The orientation of the single crystal surface was within 10° of the [0 0 1] plane. The specimens, measuring 3 mm × 6 mm and 0.4 mm

* Corresponding author. Tel.: +1-416 667 7891; fax: +1-416 667 7799.
E-mail address: michael@starfire.utias.utoronto.ca (M. Poon).

0022-3115/03/$ - see front matter
PII: S0022-3115(02)01445-9

thick, were mechanically polished and electro-polished prior to each implantation, removing approximately 3–6 μm from the surface. With this polishing treatment, it was expected that the previous implantation zone would be removed, thus eliminating any memory or hysteresis effects [1]. In most of the experiments, the specimens were then annealed at 1775 K for 30 min (5 K/s heating rate, 1 K/s cooling rate), with background pressures of 10^{-5} Pa. This anneal temperature is less than half the melting temperature for tungsten (3680 K), so it is unlikely that point defects or dislocations will be removed entirely, especially from the bulk. However, the temperature is high enough to remove any electro-polish residue from the surface, as well as some impurities, vacancies and dislocations in the near surface that were not removed by the electro-polish, and to reduce the dislocation content in the bulk [2,3]. A higher temperature anneal (2200 K for 2 min, with a background pressure of 2.5×10^{-5} Pa) was performed on two specimens in an attempt to reduce the impurity content in the bulk. The present results were compared to those of a lower purity Johnson–Matthey single crystal tungsten specimen (JM-SCW) [4]. The JM-SCW had the same crystal orientation as the M-SCW, but had 10 times higher O and C bulk impurities. Also, the JM-SCW was only annealed to 1400 K for 2 min and had a noticeably rougher surface than the M-SCW due to differences in polishing paper and electro-polishing parameters.

2.2. D^+ implantation

All implantations were performed in an ultra-high vacuum accelerator facility using D_3^+ ions at normal incidence to the test specimen. The background pressure was typically 10^{-5} Pa with the D_3^+ beam off, and 6×10^{-5} Pa (mainly D_2) during implantation. A liquid N_2 (LN_2) cold finger was installed in the specimen target chamber to reduce the hydrocarbon and water partial pressures and thus maintain a cleaner surface during implantation. In order to reduce the spatial beam flux variations, only the central part of the beam was allowed to impact on the specimen. This was achieved by clamping a W foil mask with a 2.0 mm diameter aperture in front of the specimen. A ceramic heater clamped behind the specimen was used to heat it to the selected implant temperature. A chromel–alumel thermocouple positioned between the specimen and a mica insulator, within 0.5 mm of the beam spot, was used to measure the specimen temperature during the implant.

1.5 keV D_3^+ ions (500 eV/D^+) were implanted with a flux of $5–6 \times 10^{19}$ D^+/m^2 s. Since no microstructural evolutions were observed with low energy ($\leqslant 2$ keV) H^+ irradiation [5], irradiation with 500 eV D^+ should not create defects in tungsten. In order to maintain large flux densities during implantation, a 2.5 keV D_3^+ beam was utilized, with the specimen biased to +1000 V to decelerate the beam. Here we denote the incident particle as D^+, although not all of the D particles are charged in the D_3^+ ion.

2.3. Thermal desorption spectroscopy

To ensure that the mask did not interfere in the desorption phase of the experiments, thermal desorption spectroscopy (TDS) was performed in a separate vacuum system, with delays of >8 h between implantation and desorption. The TDS system was baked for about 1 h at 400 K, giving base pressures of 2.5×10^{-6} Pa after several hours of cooling. In the baked TDS system, the main background component was D_2 from a D_2 calibrated leak bottle (50%), with water constituting the secondary component (25%). During TDS, a resistively heated W foil cradle was used for heating the implanted specimen, and its temperature was measured with a 76 μm W–5%Re/W–26%Re thermocouple spot-welded onto the specimen. Temperature ramping rates during TDS were 4–6 K/s, with a maximum temperature of 1775 K held for 5 min, and a 2 K/s post-TDS cooling rate.

D retention in the specimen was determined by integrating the Hiden Analytical quadrupole mass spectrometer (QMS) signals for D_2, HD, and D_2O during TDS. The QMS was calibrated in situ at the start of each TDS run using a D_2 calibrated leak bottle. The relative sensitivity of H_2 to D_2 was checked periodically using H_2 and D_2 calibrated leaks. The QMS library value was used for the relative sensitivity of H_2O to H_2. Due to the size of the background D_2 leak signal, the D_2 leak bottle was closed during thermal desorption. The sensitivity to HD was assumed to be the average of the H_2 and D_2 sensitivities, and the sensitivity to D_2O was assumed to be the same as for H_2O.

3. Results and discussion

3.1. SIMS surface analysis prior to D^+ implantation

Secondary ion mass spectrometry (SIMS) depth profiles were obtained for specimens at various stages of the experiment, in order to investigate the possible role of impurities on D retention. For SIMS, a 25 keV Ga^+ analysis beam was used in conjunction with a 3 keV Cs^+ sputter beam for depth profiling, with background pressures of about 3×10^{-7} Pa. The as-received M-SCW had an elevated level of O near the surface, with a lower bulk concentration. After the specimen was annealed to 1775 K for 30 min, the higher surface O content was all but eliminated and the bulk O was reduced by 50%. This suggests that the 1775 K anneal caused O to escape from the surface and near-surface of the specimen. After annealing to 2200 K for 2 min, the O^- yield increased by

3–10 times near the surface, dropping slowly with increasing depth, but never dropping below the level of the as-received specimen. This suggests that raising the temperature to 2200 K caused O to load into the specimen, presumably from residual H_2O, CO and CO_2 in the vacuum system. This reversal of the effect of annealing on surface impurity levels suggests that there were competing processes at work, with desorption dominating at 1775 K and impurity loading dominating at 2200 K. The residual gas (background) pressure was higher during the 2200 K anneal, which may have contributed to the loading effect. Comparing the SIMS O^- profiles, it was seen that the 2200 K anneal of the M-SCW specimens raised the near-surface oxygen content to nearly the same level as that of the less pure JM-SCW.

Similar trends were observed for carbon, except that the SIMS C^- ion yield was about an order of magnitude less than the O^- ion yield. Although the impurity levels were expected to be about the same, it was possible for the particular SIMS instrument to be more sensitive to oxygen than carbon. (Note that the SIMS yields have not been calibrated, and do not represent absolute concentration levels.)

3.2. SIMS surface analysis subsequent to D^+ implantation

SIMS traces are shown in Fig. 1 for: (a) an M-SCW specimen that was polished, then annealed at 2200 K for 2 min; (b) the same specimen after implanting 10^{24} D^+/m^2 at 500 K; and (c) the same specimen after TDS. After the implant, all of the elements profiled had gained a near-surface peak, which corresponds roughly to the implant zone for the D^+ ions (Fig. 1(b)). It is worth noting that beyond the O and C peaks, the impurity levels were higher than in the un-irradiated specimen, even at depths of 90 nm. The diffusivity of carbon in tungsten is normally quite small at 500 K [11], so that the diffusion length would be less than 1 monolayer. However, carbon can become much more mobile during D^+ implantations [6]. It appears that the D^+ implantation has enhanced O and C diffusion from the surface into the bulk. Since the 500 eV D^+ energy was too low to create tungsten vacancies, the enhanced diffusion was attributed to lattice strain and dislocations caused by the high mobile concentration of deuterium in a material with very low hydrogen solubility [7]. After TDS (during which the specimen was heated to 1775 K) the impurity concentrations were reduced to levels slightly less than those present after the initial 2200 K anneal (compare Fig. 1(a) and (c)).

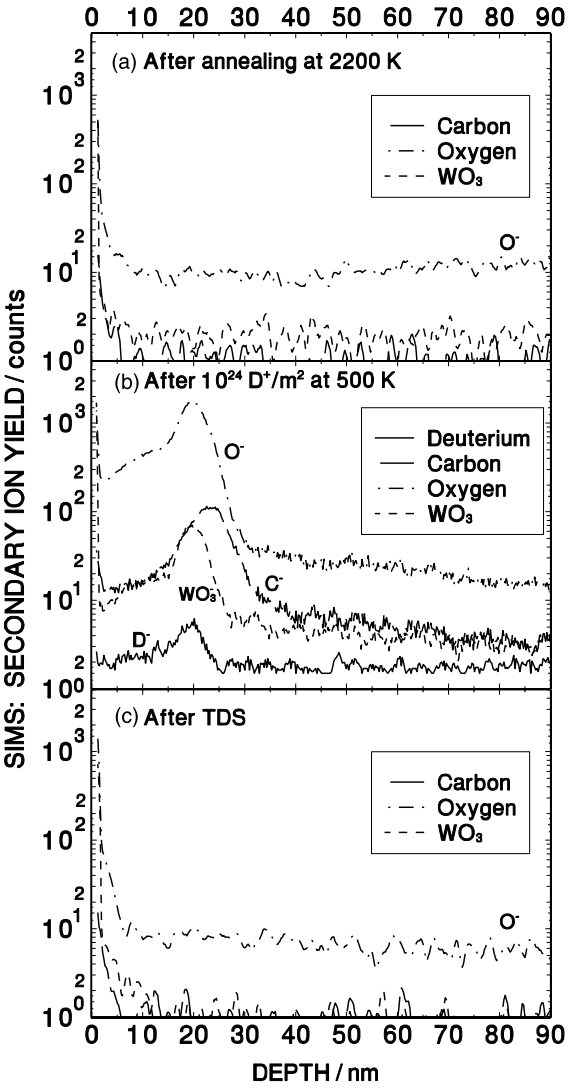

Fig. 1. SIMS profiles of M-SCW specimen showing the evolution of surface and bulk impurities after: (a) annealing at 2200 K; (b) implantation to 10^{24} D^+/m^2 at 500 K; and (c) thermal desorption at 1775 K.

3.3. Deuterium retention

Fig. 2 shows the fluence dependence of D retention in M-SCW after a 1775 K anneal followed by implantations at 300 and 500 K. For comparison, the trends for D retention in a slightly less pure JM-SCW specimen are also plotted [4]. The retention is higher for the JM-SCW after 300 K implantations to fluences $< 10^{22}$ D^+/m^2; and also after 500 K implantations to fluences $< 10^{24}$ D^+/m^2. Furthermore, the slopes of the retention curves for the two different materials are significantly different. These differences might be associated with the fact that the JM-SCW contains about 5000 appm of C and O, compared to about 500 appm of C and O in the M-SCW (according to the manufacturers). The JM-SCW specimen also underwent a lower quality surface polish and lower temperature anneal.

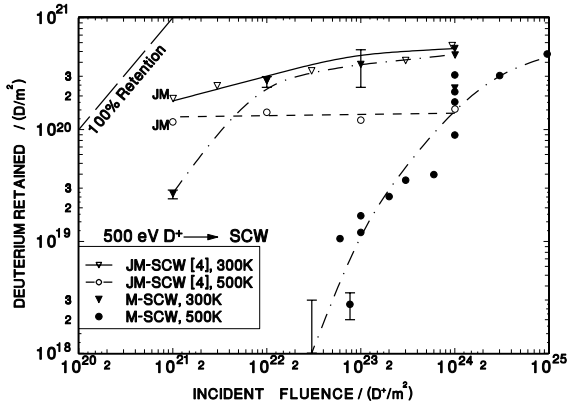

Fig. 2. D retention in M-SCW annealed at 1775 K as a function of fluence at 300 and 500 K. Previous results with lower purity JM-SCW annealed at 1273 K and a lower quality surface polish are included for comparison [4].

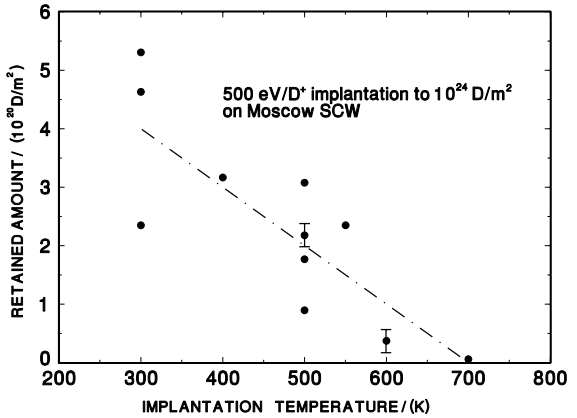

Fig. 3. Temperature dependence of D retention in M-SCW annealed at 1775 K before implantation at a fluence of 10^{24} D^+/m^2.

The temperature dependence of D retention in M-SCW at a fluence of 10^{24} D^+/m^2 is shown in Fig. 3, for $T = 300$–700 K. Deuterium retention decreased with increasing temperature, with no indication of a peak or plateau in the temperature dependence, as seen with polycrystalline tungsten and lanthanum-oxide doped tungsten [8]. No retention was observed in specimens implanted at temperatures above 700 K. The large scatter in the data, above that of the uncertainty in the measurements, may be a result of varying levels of background impurities during implantation. If D trapping were governed by the diffusion of impurities from the surface, as suggested below, then the trapped inventories may be quite sensitive to the background impurity concentrations during implantation. Unfortunately, a residual gas analyzer was not available during irradiation to monitor the background gas components.

Thermal desorption spectra for deuterium implanted at 500 K to various fluences $\leqslant 10^{24}$ D^+/m^2 exhibit a single primary peak at about 900 K (see Fig. 4(a)). For the two highest fluences ($>10^{24}$ D^+/m^2) the spectrum splits into two main peaks, one at about 900 K and one at 770 K, with two considerably smaller contributions at about 600 and 680 K. Since the lower temperature traps became populated only with the higher fluence irradiations, these trapping sites may have been ion-induced and were only accessible after a high fluence irradiation. A possible trapping scenario consists of initial trapping of deuterium at impurity or defect sites intrinsic to the specimen with a trap energy corresponding to the 900 K desorption peak. As the concentration of deuterium in the tungsten specimen grows well beyond its solubility limits, enhanced diffusion of O and C impurities from the surface into the bulk provides more traps with the same energy as the initial trapping sites. This caused the 900 K desorption peak to grow with fluence. As the implantation fluence and mobile concentration increases further, multiple deuterium atoms can become trapped at a single impurity site. These multiple atoms, or clusters of atoms, will be held with less energy than the singularly trapped deuterium, giving rise to the lower

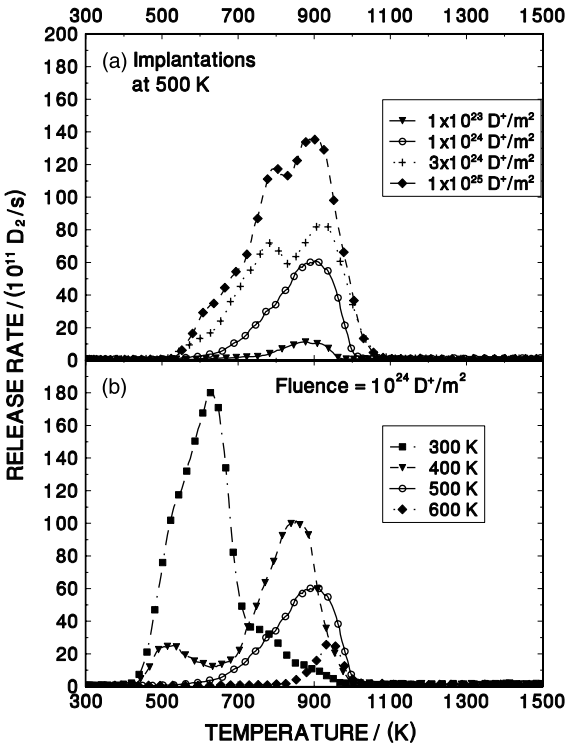

Fig. 4. TDS profiles for M-SCW annealed at 1775 K before implantation: (a) 500 K implantation temperature and various fluences and (b) various implantation temperatures at a fluence of 10^{24} D^+/m^2.

temperature, 770 K, desorption peak. As the size of the cluster grows, the trapping energy decreases, resulting in more low temperature desorption peaks with increasing fluence. With sufficient deuterium pressure, the clusters may even evolve into nano-bubbles containing D_2 molecules, with the impurity atoms acting as nucleation sites [9]. Formation of D_2 molecules in single crystal tungsten has been observed with high fluence irradiation at room temperature [10].

Fig. 4(b) shows the TDS profiles as a function of implantation temperature for a fluence of 10^{24} D^+/m^2. Two primary desorption peaks are evident: for implantation at 300 K, the primary peak occurs at 600 K, whereas for higher temperature implants, the primary peak is at 850–950 K. Two secondary peaks can be seen: one at 500 K, for the 400 K implant; and one at $\approx$750 K which contributes to all of the TDS profiles for specimens implanted at $<$600 K. The effect of temperature on the TDS profiles shows how hydrogen diffusivity affects retention. With higher temperature, the deuterium becomes much more mobile, thereby reducing the local deuterium concentration while accessing a greater volume and a greater number of intrinsic trapping sites. Thus, with the higher temperature implants, a higher fraction of the impurity traps will be occupied with only a single deuterium atom, giving rise to a high temperature primary desorption peak. At room temperature, the decreased mobility of deuterium increases the local D concentration and therefore favours multiple occupation of the trapping sites and the formation of nano-bubbles, yielding a lower temperature primary desorption peak.

4. Conclusions

SIMS and TDS results for M-SCW indicate that for 500 eV/D^+ implantation: (a) D retention increases with increasing D^+ fluence, with a clear trend to saturation for 300 K implantations; (b) D retention decreases with increasing implant temperature; (c) the trapping of D evolves with increasing fluence and temperature; and (d) C and O impurity concentrations are increased in the near-surface due to the D^+ irradiation and appear to influence the nature of traps and the amount of D retained.

SIMS measurements showed that near-surface carbon and oxygen levels decreased after annealing at 1775 K, but actually *increased* after annealing at 2200 K, and also increased after D^+ implantation. Post-implantation TDS (involving heating to 1775 K) caused a significant reduction in the near-surface C and O impurity levels.

Acknowledgements

We thank Dr Rana Sodhi, Salvatore Boccia and Fred Neub of the University of Toronto for their help with the SIMS measurements, electro-polishing and SEM measurements. We also thank Dr V.Kh. Alimov for obtaining the M-SCW specimens for us.

References

[1] A.A. Haasz, M. Poon, J.W. Davis, J. Nucl. Mater. 266–269 (1999) 520.
[2] R.A. Anderl et al., Fusion Technol. 21 (1992) 745.
[3] H. Eleveld, A. van Veen, J. Nucl. Mater. 212–215 (1994) 1421.
[4] A.A. Haasz, M. Poon, R.G. Macaulay-Newcombe, J.W. Davis, J. Nucl. Mater. 290–293 (2001) 85.
[5] R. Sakamoto, T. Muroga, N. Yoshida, J. Nucl. Mater. 220–222 (1995) 819.
[6] M. Poon, J.W. Davis, A.A. Haasz, J. Nucl. Mater. 283–287 (2000) 1062.
[7] R. Frauenfelder, J. Vac. Sci. Technol. 6 (3) (1968) 388.
[8] A.A. Haasz, J.W. Davis, M. Poon, R.G. Macaulay-Newcombe, J. Nucl. Mater. 258–263 (1998) 889.
[9] R.G. Macaulay-Newcombe, A.A. Haasz, M. Poon, J.W. Davis, in: Hydrogen and Helium Recycling at Plasma Facing Materials, Kluwer Academic, Dordrecht, 2002, p. 145.
[10] V.Kh. Alimov, K. Ertl, J. Roth, K. Schmid, Phys. Scr. T 94 (2001) 34.
[11] A.Y. Nakonechnikov, L.V. Pavlinov, V.N. Bikov, Fiz. Metal I Metalloved 22 (1966) 234 (as quoted in CRC Handbook).